

https://dspace.org/

Investigation of extended and localised states in a high-temperature superconducting ceramic.

De Villiers, Patrick

2015-03-05
http://hdl.handle.net/10539/17156

Downloaded from a DSpace repository. https://dspace.org/

2.3 Analog to Faraday's Induction Disc

In the bar sample geometry (Figure 2.3a overleaf), with the x,y directions along the length and width, respectively, an applied current density in the x direction injected at contact pair (1,2), and magnetic field directed in the z direction, will result in an electric field generated between contact pair (3,4). In the mixed state of high–T_c's the voltage detected between contact pair (3,4) is a sum of two components. A voltage contribution, W_φ resulting from the motion of localised core states, perpendicular to the applied current, is dependent on the contact separation Δ_{34}. The same dependence on Δ_{34} is valid for the contribution of the extended quasi–particle states in motion parallel to the current. In high–T_c's the Hall angle is very small[60] and flux move with an average velocity $\bar{v}_\varphi$ in a direction that can be regarded as parallel to the excitation Lorentz force. The individual contributions cannot be separated by changing magnetic field or applied current direction. The total electric field, W, generated between contact pair (3,4) is dependent on the distance separating contacts, however both contributions have the same functional dependence on this distance. Another disadvantage of this arrangement for the study of dissipative vortex flow is the exchange of entropy at the sample boundaries. Local temperature gradients can occur at the extremes of the sample due to the creation and annihilation of vortices, (see section 1.2.3).

To overcome the above obstacles of the bar geometry, it is suggested to study vortex motion in an appropriate Corbino disc–shaped sample similar to that of Faraday's induction disc experiment. By applying an electric field radially, flux motion is induced in a circular pattern (ω_φ), around the centre of the disc. This is analogous to the rotation of a conductor in a constant magnetic field, however, the functional dependence of the induced voltage contributions differ in this geometry and can be separated with suitable analysis. Also, the thermal gradients produced in the bar sample are removed in the disc geometry

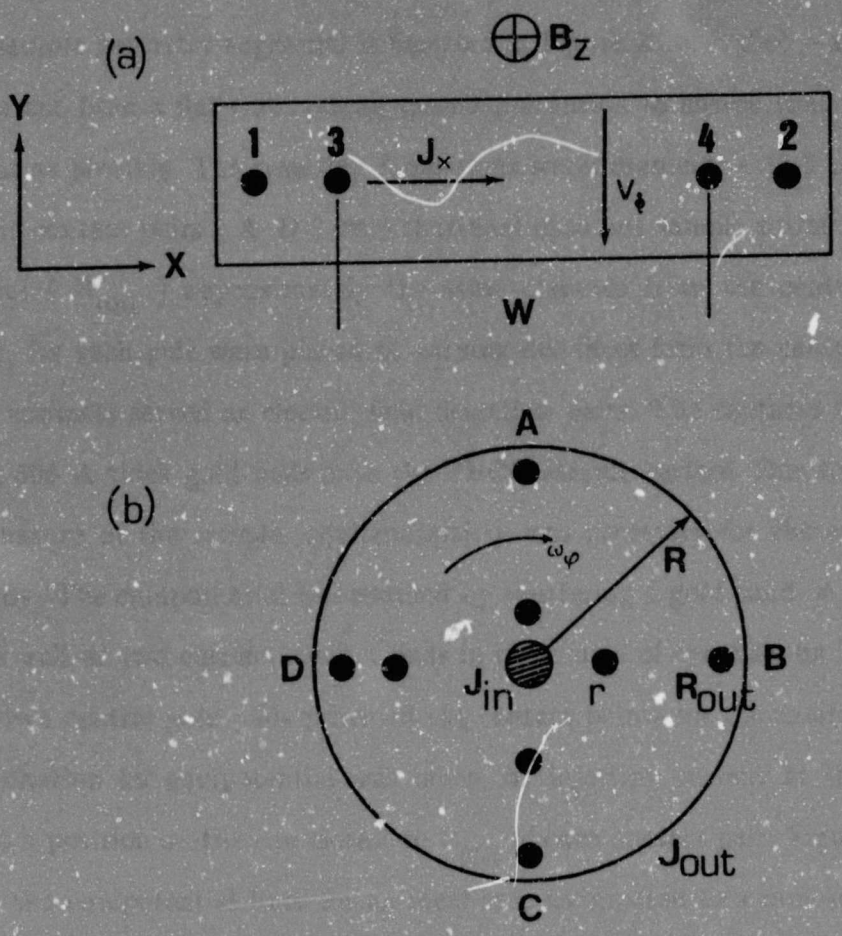


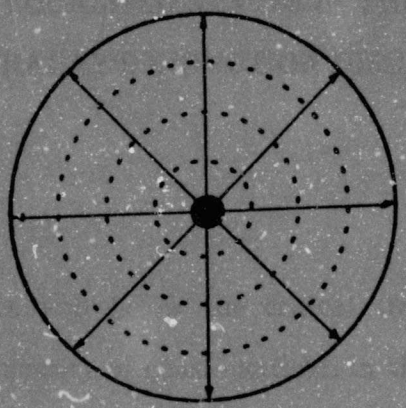
Figure 2.3

(a) A superconducting bar sample with current applied in the x–direction, between contact pair (1,2) and tranverse magnetic field in the z–direction. An electric field is detected between pair (3,4) due to the normal quasi–particle diffusion along the x–direction and also because of the motion of vortices in the y–direction.

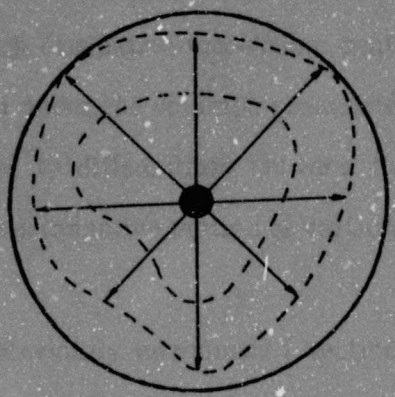
(b) A disc shaped Corbino geometry, with the current injected at the centre of the disc and removed from the rim. The four contact pairs A – D detect a radial voltage drop due to the circulating vortices as well as the radial quasi–particle motion.

since the rotating flux in a perfectly circular disc does not cross any sample boundaries. The original sample geometry suggested is depicted in Figure 2.3b. A disc – shaped sample of YBCO was cut from a flat slab, taking special precaution to ensure that the outer rim was as circular as possible. The resulting dimensions were: diameter ± 11.2 mm, thickness ± 1 mm . Four contact pairs (A–D) were sputtered onto one sample surface, all with the outside contact (R_{out}) approximately the same distance from the centre. The inner contacts (r), for each pair were placed at varying distances form the centre of the disc. These sets of contacts served as electric field detection pairs. The contacts were prepared by sputtering 500 Å thick gold pads onto the YBCO sample surface. Due to the granular weak – link nature of the sample, equipotentiality was necessary for the success of this particular study. The equipotential was ensured by sputtering a gold band on the outer rim of the disc, as well as two current contact pads in the centre of the disc, on both surfaces. The rim and two central gold pads provided the contact points for the excitation current. A further precaution for equipotential was taken, by injecting current at the centre and removing it at a position on the rim closest to R_{out} of each contact pair. Figure 2.4 depicts schematically the equipotential lines for an ideal case as opposed to a non–ideal situation most likely to occur in experimental procedures. The boundary lines can be regarded as 'iso–currents' where the current strength remains the same around the sample.

The analysis and functional dependence of the induced voltage at the voltage pair contacts is discussed in the following chapter (Chapter 3), along with the results for the Activation Energies corresponding to the above implied current induced Proximity Effect.



IDEAL



NON-
IDEAL

Figure 2.4

A schematic representation of the equipotentiality for an ideal disc geometry and non-ideal case. The connecting concentric lines can be regarded as "iso-currents" showing the possibility for irregular current densities in the experimental sample.

CHAPTER 3

EXTENDED AND LOCALISED STATES IN THE ANALOG TO FARADAY'S INDUCTION DISC

3.1 Introduction

The existence of extended states well below the critical transition temperature, T_c, suggests that there exist a finite density of quasi–particles in the energy gap of High–T_c superconductors. The dissipation of the high–T_c in the mixed state is composed of a dual contribution from the localised core states and extended quasi–particle states. The fractions of dissipation to which each dissipative mechanism contributes has not been clear in previous studies of vortex motion under the common geometries applied. A novel sample geometry and analysis is suggested to differentiate between the resistive quasi–particle scattering processes and the tranverse inductive motion of vortices.

The geometry proposed has been previously introduced (section 2.3, see figure 2.3b). A linear relation is assumed for the two contribu ons, W_N and W_φ, which form the total radial voltage, W.

$$W = W_N + W_\varphi \qquad 3.1.$$

This assumption is plausible, based on Faraday's Law of Induction for rotating circuits within a magnetic field, where the total induced electric field is a linear sum of the closed circuit electric field and the induced electric field: $E = E_C - (v_\varphi \times B)$[61].

The quasi–particle contribution, $W_N = \alpha_q w_n$, where α_q is the fraction of the normal state contribution, w_n, when the vortex induced contribution has been removed. The electric potential, w_n, is due to the usual flow of normal carriers in the direction of the radial current density. It is expected to have the following form:

$$w_n = I \cdot d(R) \cdot \rho_N(T) \qquad 3.2$$

where I, is the radial current applied to the disc, d(R), is a function describing the radial dependence of the voltage contribution between the two contact points and $\rho_N(T)$, is the normal state resistivity extrapolated in the linear region, ($T > 90$ K) for the resistivity curves of each contact pair. The extrapolation for $\rho_N(T)$ is performed well above any fluctuation important region[54]. The electric field generated between the contact points in a pair is proportional, (α), to the inverse distance separating them; namely, $\mathbf{E} = \rho \cdot \mathbf{J}$, for a radial current density, and $J \alpha 2\pi/R$ implies $E \alpha 2\pi\rho/R$. From $E = -\partial V/\partial R$ and integrating between the contact pair (R_{out}, r),

$$\int_r^{R_{out}} \frac{1}{R} dR \ \alpha \, w_N \qquad 3.3.$$

Hence, d(R) has the following form, $d(R) \equiv \log(R_{out}/r)$[62].

The voltage contribution, W_φ, due to induction via the circulating vortices has the general form,

$$W_\varphi = D(R) \cdot \Gamma_\varphi(T,J,B) \qquad 3.4$$

where $\Gamma(R)$ represents the radial dependence for this contribution, and Γ_φ is proposed to depend on the magnetic field, B, the current, J and a characteristic rate for the rotating

vortices, ν_{eff}. The temperature dependence of Γ_φ is analysed in accordance with the TAFF model below. The radial function D(R) is formulated with the aid of Anderson's theory of Phase slip in vortices[63], (see figure 3.1). For moving vortices with some frequency a voltage is induced between the contact pairs because of the phase difference at the contacts. If n vortices cross the line connecting the contacts, (in unit time), then a voltage, $W = \varphi_o \cdot n$ is induced. The fraction of vortices involved in the generation of the electric field are $n = (N \cdot \Delta S)/(S \cdot \tau_{eff})$ where N is the total number of mobile vortices, and $S = \pi R_{out}^2$, the total surface for mobile vortices and $\Delta S = \pi(R_{out}^2 - r^2)$ the surface between the contacts involved. τ_{eff} is an effective time for the vortices to cross the contact line. Therefore, using the fact, $B = \varphi_o \cdot N/S$ we have that the voltage generated is:

$$W_\varphi = B \cdot \frac{1}{\tau_{eff}} \cdot (R_{out}^2 - r^2) = B \cdot \nu_{eff} \cdot (R_{out}^2 - r^2) \qquad 3.5.$$

In analogy to Faraday's induction disc, (for a Normal metal) the electric field induced between two concentric circles will be linear in R, the distance between them. For that case, integrating between two contact points (R_{out}, r) provides the radial dependence for $D(R) \equiv (R_{out}^2 - r^2)$.

The different dependencies on R, are the essence of this analysis and hence enable the two contributions to be separated. By substituting the radial dependence, D(R), for W_φ, into equation 3.4 and manipulating equation 3.1 it follows that the radial voltage drop for each contact pair can be expressed as,

$$W/w_n = \alpha_q + (R_{out}^2 - r^2) \cdot \Gamma_\varphi / w_n \qquad 3.6.$$

W is the measured voltage between the contact pairs for both contributions and w_n is found from the normal–state extrapolation, (see equation 3.2 above).

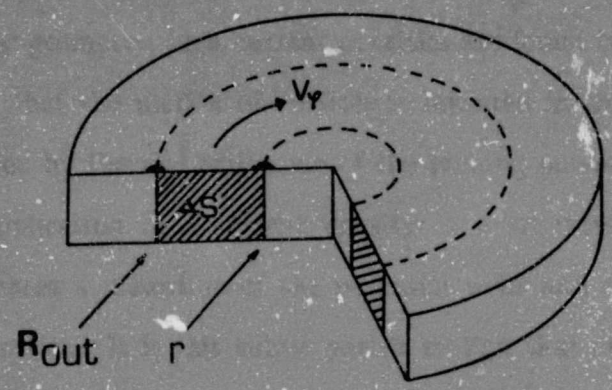


Figure 3.1 Corbino sample geometry displaying a typical contact pair, (R_{out}, r). A section of the sample geometry has been removed to illustrate the radial dependence of W_φ deduced from Anderson's model of Phase slippage.

By plotting W/w_n versus $(R_{out}^2 - r^2)/w_n$ and fitting a straight line to the data for four contact point pairs, the corresponding value of α_q can be found from the intercept of the line formed when $R_{out} = r$. The value of $\alpha_q(T)$ lies in the interval, $0 \leq \alpha_q(T) \leq 1$ and $\alpha_q \rightarrow 1$ for $T > T_c$. The induced term, Γ_φ, is found by the same procedure: Γ_φ is the gradient of the straight lines produced for each discrete temperature. This procedure ensures that an averaged value of Γ_φ is found for all the four contact pairs.

The analysis is extended to the temperature dependence of Γ_φ, the dissipation due to mobile vortices. In the disc geometry, high current densities are found in the centre of the disc, hence it is expected that the motion of vortices is initiated in this area due to the stronger Lorentz force aided by thermal activation of the pinning potentials. As discussed extensively above, the application of a current density in a tranverse direction to an applied magnetic field, causes a distortion of the potential wells and thermal activation leads to the hopping of vortices. It is this subtle vortex motion that eventually develops into a state of flux flow. In the analysis above, the dissipation due to this vortex motion from its onset, is related directly to the value of Γ_φ. The theory of TAFF (see section 1.2.4.3) is particularly suited in dealing with Γ_φ as all contributions from extended excitations are removed. Also, the current regime that was measured is in the low current limit for the analysis in terms of TAFF.[48,49,51] The expression for thermally activated flux flow in the low current regime is a function of the activation energy and the flux flow resistivity,

$$\rho_{TAFF} = S^* \rho_{FF} \, U/k_B T \exp(-U/k_B T) \qquad 3.7$$

where S^* is dependent on the shape of the pinning potential, $\rho_{FF} = \rho_N B/H_{c2}(T)$ and U has the form given by equation 1.2.8. Krause et al[50], fit the above expression to the resistivity data of $Bi_2Sr_2CaCu_2O_y$ crystals, up to temperatures where the flux flow term

becomes predominant. For this specific study the general TAFF expressions are modified to suit the special case described below. As mentioned above, the experimental set–up used, caused higher current densities to occur in the centre of the disk than at the edges, for example. The non–ideal current distribution through the sample has the effect of producing inter – granular normal regions in contact with superconducting regions, (N–S junctions). These intrinsic boundaries are formed when the current density is large enough to break the weak links that are formed due to the lack of oxygen stoichiometry in the sample. This is referred to as **intrinsic Proximity boundaries**, where proximity effects such as pair breaking and Josephson Cooper–pair tunneling occur. These intrinsic N–S boundaries form suitable sites for the thermal activation of flux creep. Therefore an analytical fit to the data of Γ_{φ} is performed using the extended Proximity – Mediated TAFF expression, (PMTAFF),

$$\Gamma_{\varphi} = [\Gamma_o(J,B)\cdot U(T,B)]\exp[-U(T,B)] \qquad 3.8$$

for temperatures up to $T_c(H)$, defined as the temperature corresponding to the peak in the temperature derivative of the W(T) curves for the contact pairs, where,

$$U(T,B) = U_o \exp[-B/B_o]\cdot[1-t^2]^{3/2} \qquad 3.9$$

and $t \equiv T/T_c(H)$, the reduced temperature. For a discussion on the intrinsic proximity mediated flux flow and derivation of the above results, as well as an alternative form for the activation energy, see APPENDIX A.

The theoretical expression, 3.8, is fitted by considering $\log(\Gamma_{\varphi})$ and $1/T$ as the dependent and independent variables, respectively, in a Least Squares Approximation. $\Gamma_{\varphi}(T)$ imitates a broad Gaussian form with its peak value at, (or just below), the $T_c(B)$ value for the respective voltage curve. In figure 3.2, a normalised voltage curve, ($W(T)/W(T = 90\ K)$),

and $\Gamma_{\varphi}(T)$ normalised to its peak value, are superimposed to indicate the region in which the extended TAFF theory is fitted. Although the Least Squares Fit provides an error in the fit corresponding to the adjusted variables (i.e. $\log(\Gamma_{\varphi})$), it does provide a good indication of the relevant temperature interval in which the fit is most successful. For the sake of consistency, the temperature interval for the fit considered is usually taken as the temperature point just below $T_c(B)$, to the first two temperature points that enter the noise level at the base of the $\Gamma_{\varphi}(T)$ curve. From the fit, two parameters are found, **U(B)**, the field dependent activation energy and $\Gamma_o(J,B)$, the temperature independent constant, (see APPENDIX A). $\Gamma_o(J,B)$ is proportional to $J \cdot B^{1/2} \exp[-B/B_o]$ and is proportional to the effective rate of the rotating vortices, ν_{eff}

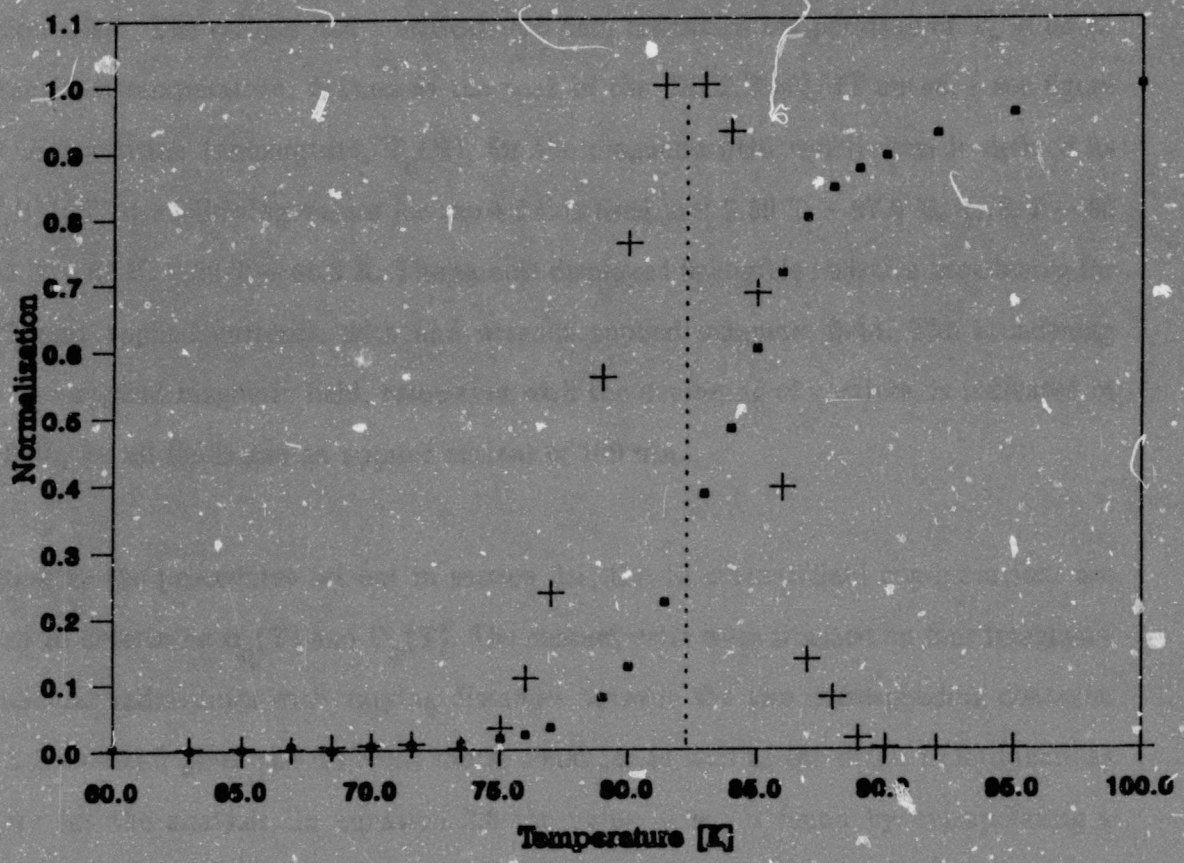


Figure 3.2 A typical voltage curve, W(T), [·] superimposed with its respective $\Gamma_{\varphi}(T)$, [+] curve to indicate the region in which the PMTAFF theory is fitted. The W(T) curve is normalised as, [W(T)/W(100 K)] and $\Gamma_{\varphi}(T)$ normalised to its peak value.

Author De Villiers P
Name of thesis Investigation of extended and localised states in a high-temperature superconducting ceramic 1994

PUBLISHER:
University of the Witwatersrand, Johannesburg
©2013

LEGAL NOTICES:

Copyright Notice: All materials on the University of the Witwatersrand, Johannesburg Library website are protected by South African copyright law and may not be distributed, transmitted, displayed, or otherwise published in any format, without the prior written permission of the copyright owner.

Disclaimer and Terms of Use: Provided that you maintain all copyright and other notices contained therein, you may download material (one machine readable copy and one print copy per page) for your personal and/or educational non-commercial use only.

The University of the Witwatersrand, Johannesburg, is not responsible for any errors or omissions and excludes any and all liability for any errors in or omissions from the information on the Library website.